Simultaneous Reception and Sensing using Multiple Antennas in Cognitive Cellular Networks

Prasanth Karunakaran*, Thomas Wagner†, Ansgar Scherb†, Aylin Solak*, and Wolfgang Gerstacker*
*Institute for Digital Communications
Friedrich-Alexander-University Erlangen-Nürnberg (FAU), Germany
Email: {karunakaran,gersta}@lnt.de
†Ericsson, Nürnberg, Germany
Email: {thomas.wagner,ansgar.scherb}@ericsson.com

***Abstract*—We consider the problem of sensing in the presence of a desired signal in the context of future 3GPP LTE-A based cognitive cellular systems employing multiple-input multiple-output (MIMO) transmission. Energy detection (ED) based on equal gain combining and beamforming are investigated. Receive beamformers for energy detection (ED) are designed according to the Neyman-Pearson criterion to maximize the probability of detection for a given probability of false alarm. Suitable suboptimum solutions to the maximization problem with a good tradeoff between performance and complexity are identified. Furthermore, we also formulate the likelihood ratio test (LRT) for this scenario. Performance simulations indicate that a significant performance gain is achieved in ED if the receive beamformer is chosen properly.**

I. INTRODUCTION

It has been well established in the literature that the fixed spectrum allocation in traditional wireless systems results in a low spectrum utilization. The quest to achieve a higher spectrum efficiency has driven the development of the cognitive radio (CR) technology which opportunistically exploits the unused resources of an existing system with fixed spectrum allocation [1][2]. In the CR literature, the users of the fixed spectrum allocation based system and the opportunistic users of the CR system are referred to as primary users and secondary users or CR users, respectively, and the opportunistic access is also referred to as dynamic spectrum access (DSA). As a primary system is already existing, it is unaware of the existence of the secondary users and hence the secondary users must ensure that the interference to the primary system stays below the acceptable level. However, future systems may be designed according to a different paradigm, where all users are CR users with equal or different priorities. There are scenarios where DSA can be beneficial for cellular networks. An example is the sharing of spectrum between different cellular operators. Spectrum sharing is advantageous as it enables a lightly loaded network to share a portion of its spectrum with another operator who is in need for additional resources. Such an arrangement has the potential to improve both the spectrum utilization and the profitability. A corresponding business model has attracted interest recently [3][4][5]. In this work, we consider spectrum sharing in 3GPP LTE-A systems [6].

Carrier aggregation (CA) is an important feature of LTE-A that was introduced to enable very high data rates [6]. This is achieved by increasing the available bandwidth up to 100 MHz by aggregating up to five component carriers of 20 MHz bandwidth each. Spectrum acquisition being highly capital intensive to an operator, the increased capacity provided by CA is beneficial only if there is a sufficient demand of the users. Depending on the load, an operator could possibly use one or more component carriers in a spectrum shared manner with another operator. In [5] we have investigated the possibility of spectrum sharing in LTE-A systems with CA where the cross-carrier scheduling of LTE-A and sensing are identified as key enablers. Here, cross-carrier scheduling allows the physical downlink shared channels (PDSCHs) in a component carrier to be scheduled by a physical downlink control channel (PDCCH) of another component carrier. This helps to overcome one of the important impediments in a spectrum shared operation arising from the LTE-A control channel frame structure. In LTE-A, the PDCCHs must be transmitted within the first three OFDM symbols of a subframe and are spread across the entire bandwidth. Transmitting PDCCHs by both operators on the shared carrier would inevitably result in control channel collisions. If one of the operators has another exclusive component carrier, transmitting its PDCCHs via this carrier avoids the control channel collisions. PDSCHs which are frequency domain scheduled are not prone to such problems and are well suited for a spectrum shared operation. Due to these reasons, LTE-A is a suitable candidate for a spectrum shared operation.

Sensing is performed by the CR users to determine a possible activity in a time-frequency resource. The possibilities for the granularity of spectrum sharing in LTE-A and its implications on sensing are discussed in [5], where the spectrum sharing is classified into long-term sharing and short-term sharing and the sensing is categorized into Type 1 sensing and Type 2 sensing. Here, Type 1 sensing is performed before the transmission to determine whether a spectral band is occupied or not. The majority of the CR literature on sensing deals with Type 1 sensing [7]. In Type 2 sensing, a user senses the activity of the other users while its communication already takes place. Type 2 sensing can be posed as a hypothesis testing problem where the competing hypotheses are the "serving cell signal + noise" (H_1') hypothesis and the "serving cell signal + interfering signal + noise" hypothesis (H_2). In this work, we consider Type 2 sensing in the short-term spectrum sharing scenario of [5], where spectrum is shared with the smallest possible granularity of a physical resource block (PRB), which consists of 12 subcarriers and 14 OFDM symbols and occupies a 1 ms$\times$180 kHz slice of the time-frequency plane. Recently, this problem of sensing in presence of a desired signal has been addressed in [8][9]. In [8] the

This work has been performed in the framework of the Cognitive Mobile Radio (CoMoRa) project, which is partly funded by the Federal Ministry of Education and Research (BMBF) of Germany.

CROWNCOM 2014, June 02-04, Oulu, Finland

DOI 10.4108/icst.crowncom.2014.255096

authors proposed zero-forcing beamforming by the secondary base station towards idle secondary users who can then sense as if there is no secondary signal. In [9] a multiple-input multiple-output (MIMO) system is considered with pre- and post-processing based on singular value decomposition (SVD) of the channel matrix to decompose the system into parallel subchannels. The transmit power, the sensing time and the sensing threshold in each subchannel are optimized to maximize the CR throughput under a constraint for the probability of false alarm and detection. These two approaches are not directly applicable to LTE-A systems, because the transmission modes and precoding are standardized and sensing must adhere to these restrictions. Therefore, in [5], we have studied energy detection (ED) and likelihood ratio test (LRT) for an LTE system with single-input single-output (SISO) transmission. In this paper, we extend our previous work to a multiple-input multiple-output (MIMO) configuration. The main focus is on energy detection. Even though energy detection requires an accurate estimate of the noise variance, it remains popular because of its low computational complexity. The additional degrees of freedom provided by multiple receive antennas can be exploited for improving the detection performance. We extend the equal gain combining method of [10] for Type 2 sensing and develop a beamforming based energy detector. The Neyman-Pearson (NP) criterion of maximizing the probability of detection for a target probability of false alarm is used for the beamformer design. Beamformers that provide significant performance gains are identified. We also study the impact of channel estimation errors on the various solutions. Finally, we formulate the LRT for the MIMO scenario. We note that, even though sensing is described in the context of spectrum sharing between operators, such a capability may find use also in the device to device (D2D) communication scenario in LTE-A.

The paper is organized as follows. Section II describes the system model for the short-term sensing scenario. In Section III the energy detectors based on equal gain combining and beamforming, respectively, are formulated and analyzed. In Section IV we state the likelihood ratio test, and simulation results are presented in Section V. Section VI provides the conclusion.

II. System Model

Consider a spectrum sharing system with two 3GPP LTE-A base stations, BS1 and BS2, belonging to two different network operators as shown in Figure 1. The operators are expected to have made certain agreements on spectrum sharing related to pricing, time scale of sharing, amount of tolerable interference caused to each other, etc. We study the downlink scenario where sensing is performed by the user equipment (UE) or dedicated sensing equipments installed by the operators. This is a reasonable assumption because it is the UE which is affected by downlink interference, and the base station is usually not equipped with a downlink receiver. The sensing result could be reported back to the serving base station via uplink messaging which controls the sensing and reporting. For example, the base station might instruct certain UEs to do sensing on particular PRBs or subframes. It is also assumed that the base station informs the selected UEs about whether the PRBs or subframes to be sensed carry the base station's transmissions or not. This assists the UE to determine which test to perform when the PRBs are not allocated for UE's own

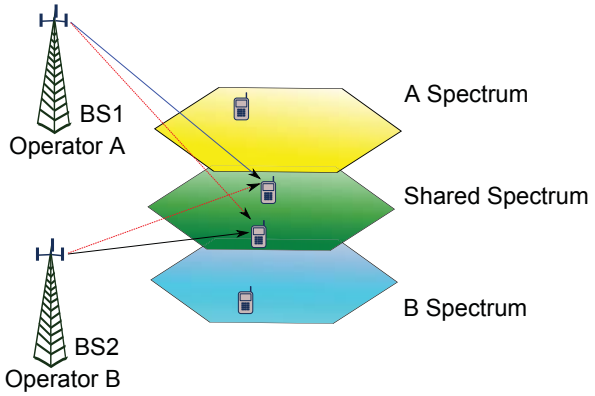

Fig. 1. Spectrum sharing between two base stations

transmission. If the serving cell's signal is not present, the UE performs the Type 1 sensing.

For the remainder of the paper, we consider Type 2 sensing from the perspective of a BS2 user trying to detect the activity of BS1. BS1 and BS2 are equipped with N_{T1} and N_{T2} transmit antennas and the BS2 user is equipped with N_R receive antennas. The sensing can be posed as the following hypothesis testing problem.

$$\begin{aligned} H_1^{'} &: \mathbf{y}_k = \sqrt{\alpha_2}\,\mathbf{H}_2\mathbf{x}_{2k} + \mathbf{n}_k; && k = 1, 2, ..., N, \\ H_2 &: \mathbf{y}_k = \sqrt{\alpha_1}\,\mathbf{H}_1\mathbf{x}_{1k} + \sqrt{\alpha_2}\,\mathbf{H}_2\mathbf{x}_{2k} + \mathbf{n}_k; && k = 1, 2, ..., N, \end{aligned} \quad (1)$$

where $\mathbf{y}_k = [y_{1k}, ..., y_{N_R k}]$ represents the receive vector at resource element k, entry y_{mk} is the receive symbol at antenna m, $\mathbf{H}_i$ denotes the channel matrix between the ith BS and the UE composed of independent and identically distributed (i.i.d.) complex Gaussian random variables with unit variance. $\mathbf{x}_{ik}$ is the transmit symbol vector at resource element k of the ith BS, $\sqrt{\alpha_i}$ represents the large-scale propagation coefficient from the ith BS, N is the number of resource elements considered in sensing and $\mathbf{n}$ stands for additive white Gaussian noise (AWGN) with zero mean and covariance matrix $\sigma_n^2\mathbf{I}$. For simplicity, it is assumed that the transmit symbols of the ith BS are independent in both antenna direction and resource element index k and have an average symbol energy of $\frac{E_x}{N_{Ti}}$. The small-scale fading channel matrix $\mathbf{H}_i$ is assumed to be constant across all the considered resource elements. This is a reasonable assumption when the sensing is performed over a PRB where the channel variations are expected to be low.

As the time scale of sharing in the short-term spectrum sharing scenario is quite small, it is not possible to completely turn off the base stations which are currently not active. In LTE systems, when the base station is on, it is required to transmit different channels such as common reference channels (CRS), control channels, synchronization channels etc. even though the PDSCHs are not loaded. Since Type 2 sensing is intended to detect an activity of the PDSCH in a PRB, only the resource elements corresponding to the PDSCH should be included in the sensing process. Also, since the reference signals from both base stations are always on, it is possible to estimate their channel states. The channel state of the serving cell (BS2) is needed in any case for data decoding. Thus, we assume the availability of channel state information in the

following discussions. It should also be noted that the inter-cell interference coordination (ICIC) and enhanced ICIC in LTE-A can be made use of in the spectrum sharing if there is an X2 interface between BS1 and BS2. It is not clear if such an exchange is possible between different operators. Even if it is possible, sensing would supplement in achieving a higher flexibility as information exchange over X2 can happen only every 20 ms which is a time span already comprising 2000 PRBs in each 20 MHz carrier [6]. Also, if a cognitive operation is desired in a D2D scenario, sensing would be the only option.

The sensing/detection performance is characterized in terms of the probability of false alarm (P_f) and the probability of detection (P_d) [11] defined as

$$P_f = P(\text{Decide } H_2 | H_1^{'} \text{ True}) \tag{2}$$
$$P_d = P(\text{Decide } H_2 | H_2 \text{ True}). \tag{3}$$

III. Energy Detection

A. Energy detector with equal gain combining (ED-EGC)

EGC is designed similar to [10], but applied for distinguishing between $H_1^{'}$ and H_2, and is given by

$$\begin{aligned} e_1 &= \frac{2}{\sigma_n^2} \sum_{k=1}^{N} \sum_{m=1}^{N_R} |y_{mk}|^2 \\ &\text{Decide } H_2 \text{ if } e_1 > t_{EGC}. \end{aligned} \tag{4}$$

Given $\sqrt{\alpha_1}\,\mathbf{H}_1$, $\sqrt{\alpha_2}\,\mathbf{H}_2$, $\mathbf{x}_{1k}$ and $\mathbf{x}_{2k}$, the PDFs of y_{mk} under $H_1^{'}$ and H_2 are $\mathcal{CN}(\sqrt{\alpha_2}\,\mathbf{h}_{2m}^T\mathbf{x}_{2k}, \sigma_n^2)$ and $\mathcal{CN}(\sqrt{\alpha_1}\,\mathbf{h}_{1m}^T\mathbf{x}_{1k} + \sqrt{\alpha_2}\,\mathbf{h}_{2m}^T\mathbf{x}_{2k}, \sigma_n^2)$ respectively, where $\mathbf{h}_{im}$ is the mth column of $\mathbf{H}_i^T$. Thus, the energy e_1 involves the sum of $2NN_R$ real and independent squared Gaussian random variables. Hence the PDF of e_1 under both hypotheses is a non-central chi-square PDF $\chi_\nu^2(\lambda)$ with $\nu = 2NN_R$ degrees of freedom but different non-centrality parameters $\lambda = \lambda_1$ and $\lambda = \lambda_2$, respectively [13, Eq. 2.1.117-124].

$$\begin{aligned} H_1^{'} &: e_1 \sim \chi_\nu^2(\lambda_1) \\ \text{where } \lambda_1 &= \frac{2}{\sigma_n^2} \sum_{m=1}^{N_R} \sum_{k=1}^{N} |\sqrt{\alpha_2}\,\mathbf{h}_{2m}^T\mathbf{x}_{2k}|^2 \\ &\approx \frac{2\alpha_2 N E_x}{\sigma_n^2 N_{T2}} \sum_{m=1}^{N_R} \mathbf{h}_{2m}^H\mathbf{h}_{2m} \end{aligned} \tag{5}$$

$$\begin{aligned} H_2 &: e_1 \sim \chi_\nu^2(\lambda_2) \\ \text{where } \lambda_2 &= \frac{2}{\sigma_n^2} \sum_{m=1}^{N_R} \sum_{k=1}^{N} |\sqrt{\alpha_1}\,\mathbf{h}_{1m}^T\mathbf{x}_{1k} + \sqrt{\alpha_2}\,\mathbf{h}_{2m}^T\mathbf{x}_{2k}|^2 \\ &\approx \frac{2NE_x}{\sigma_n^2} \sum_{m=1}^{N_R} \frac{\alpha_1 \mathbf{h}_{1m}^H\mathbf{h}_{1m}}{N_{T1}} + \frac{\alpha_2 \mathbf{h}_{2m}^H\mathbf{h}_{2m}}{N_{T2}}. \end{aligned} \tag{6}$$

For large degrees of freedom, $\chi_\nu^2(\lambda)$ can be approximated by the Gaussian PDF, $\mathcal{N}(\nu+\lambda, 2(\nu+2\lambda))$. Given a channel state $\sqrt{\alpha_2}\,\mathbf{H}_2$, a false alarm occurs when the energy exceeds the threshold t_{EGC} and the corresponding probability is given by

$$\begin{aligned} P_f(t_{EGC}|\sqrt{\alpha_2}\,\mathbf{H}_2) &= P(e_1 > t_{EGC}|\sqrt{\alpha_2}\,\mathbf{H}_2, H_1^{'}) \\ &= Q\left(\frac{t_{EGC} - (\nu+\lambda_1)}{\sqrt{2(\nu+2\lambda_1)}}\right), \end{aligned} \tag{7}$$

where $Q(\cdot)$ is the Q-function. The threshold for a target false alarm probability of δ is obtained from (7) as

$$t_{EGC} = Q^{-1}(\delta)\sqrt{2(\nu+2\lambda_1)} + (\nu+\lambda_1). \tag{8}$$

The probability of detection for the channel states $\sqrt{\alpha_1}\,\mathbf{H}_1$ and $\sqrt{\alpha_2}\,\mathbf{H}_2$ is given by

$$P_d(t_{EGC}|\sqrt{\alpha_1}\,\mathbf{H}_1, \sqrt{\alpha_2}\,\mathbf{H}_2) = Q\left(\frac{t_{EGC} - (\nu+\lambda_2)}{\sqrt{2(\nu+2\lambda_2)}}\right). \tag{9}$$

B. Energy detector with beamforming (ED-BF)

In the energy detector with beamforming, detection is performed after linearly combining the receive symbols from the different antennas. The detector is formulated as follows:

$$r_k = \mathbf{w}^H\mathbf{y}_k \tag{10}$$

$$\begin{aligned} e_2 &= \frac{2}{\sigma_n^2\mathbf{w}^H\mathbf{w}} \sum_{k=1}^{N} |r_k|^2 \\ &\text{Decide } H_2 \text{ if } e_2 > t_{BF}. \end{aligned} \tag{11}$$

It can be observed that, given the channel matrices and symbol vectors, r_k is distributed as $\mathcal{CN}(\sqrt{\alpha_2}\mathbf{w}^H\mathbf{H}_2\mathbf{x}_{2k}, \sigma_n^2\mathbf{w}^H\mathbf{w})$ and $\mathcal{CN}(\sqrt{\alpha_1}\mathbf{w}^H\mathbf{H}_1\mathbf{x}_{1k} + \sqrt{\alpha_2}\mathbf{w}^H\mathbf{H}_2\mathbf{x}_{2k}, \sigma_n^2\mathbf{w}^H\mathbf{w})$ under the hypotheses $H_1^{'}$ and H_2, respectively. Thus, it can be seen that e_2 is the sum of squares of $2N$ real and independent Gaussian random variables of unit variance and non-zero mean. Hence e_2 is non-central chi-square distributed with u degrees of freedom, $u = 2N$, but different non-centrality parameters, $\lambda = \lambda_3$ and $\lambda = \lambda_4$, respectively.

$$\begin{aligned} H_1^{'} &: e_2 \sim \chi_u^2(\lambda_3) \\ \text{where } \lambda_3 &= \frac{2}{\sigma_n^2\mathbf{w}^H\mathbf{w}} \sum_{k=1}^{N} |\sqrt{\alpha_2}\mathbf{w}^H\mathbf{H}_2\mathbf{x}_{2k}|^2 \\ &\approx \frac{2\alpha_2 N E_x}{\sigma_n^2 N_{T2}\mathbf{w}^H\mathbf{w}} \mathbf{w}^H\mathbf{H}_2\mathbf{H}_2^H\mathbf{w} \end{aligned} \tag{12}$$

$$\begin{aligned} H_2 &: e_2 \sim \chi_u^2(\lambda_4) \\ \text{where } \lambda_4 &= \frac{2}{\sigma_n^2\mathbf{w}^H\mathbf{w}} \sum_{k=1}^{N} |\sqrt{\alpha_1}\mathbf{w}^H\mathbf{H}_1\mathbf{x}_{1k} + \sqrt{\alpha_2}\mathbf{w}^H\mathbf{H}_2\mathbf{x}_{2k}|^2 \\ &\approx \frac{2NE_x}{\sigma_n^2\mathbf{w}^H\mathbf{w}} \left(\frac{\alpha_1\mathbf{w}^H\mathbf{H}_1\mathbf{H}_1^H\mathbf{w}}{N_{T1}} + \frac{\alpha_2\mathbf{w}^H\mathbf{H}_2\mathbf{H}_2^H\mathbf{w}}{N_{T2}}\right). \end{aligned} \tag{13}$$

As in (8), the threshold for a target probability of false alarm of δ is calculated from the Gaussian approximation as

$$t_{BF} = Q^{-1}(\delta)\sqrt{2(u+2\lambda_3)} + (u+\lambda_3). \tag{14}$$

The probability of detection is given by the probability that the energy exceeds the threshold under hypothesis H_2, which is the right tail probability of energy under hypothesis H_2. For the threshold in (14), the probability of detection is given by

$$P_d(t_{BF}|\sqrt{\alpha_1}\,\mathbf{H}_1, \sqrt{\alpha_2}\,\mathbf{H}_2) = Q\left(\frac{t_{BF}-(u+\lambda_4)}{\sqrt{2(u+2\lambda_4)}}\right). \tag{15}$$

For a given δ, $\sqrt{\alpha_1}\,\mathbf{H}_1$ and $\sqrt{\alpha_2}\,\mathbf{H}_2$, $P_d(t_{BF}|\sqrt{\alpha_1}\,\mathbf{H}_1, \sqrt{\alpha_2}\,\mathbf{H}_2)$ is a function of the beamforming vector $\mathbf{w}$. According to the Neyman-Pearson criterion the optimum choice of $\mathbf{w}$ is the one that maximizes $P_d(t_{BF}|\sqrt{\alpha_1}\,\mathbf{H}_1, \sqrt{\alpha_2}\,\mathbf{H}_2)$ under fixed P_f. Since the Q-function is a monotonically decreasing function, the maximization of the Q-function is equivalent to the minimization of the argument of the Q-function. After substituting the values from (12), (13) and (14), the design problem for $\mathbf{w}$ can be formulated as follows

$$\min_{\mathbf{w}} \frac{Q^{-1}(\delta)2\sqrt{N+\frac{2N\alpha_2 E_x \mathbf{w}^H\mathbf{H}_2\mathbf{H}_2^H\mathbf{w}}{\sigma_n^2 N_{T2}\mathbf{w}^H\mathbf{w}}} - \frac{2N\alpha_1 E_x \mathbf{w}^H\mathbf{H}_1\mathbf{H}_1^H\mathbf{w}}{\sigma_n^2 N_{T1}\mathbf{w}^H\mathbf{w}}}{2\sqrt{N+\frac{2NE_x}{\sigma_n^2\mathbf{w}^H\mathbf{w}}\left(\frac{\alpha_1\mathbf{w}^H\mathbf{H}_1\mathbf{H}_1^H\mathbf{w}}{N_{T1}}+\frac{\alpha_2\mathbf{w}^H\mathbf{H}_2\mathbf{H}_2^H\mathbf{w}}{N_{T2}}\right)}}. \tag{16}$$

The above problem can be converted to an equivalent problem. For this, we observe the fact that the solutions are not affected by scaling. That is, $\mathbf{w} = \mathbf{w}_0$ and $\mathbf{w} = c\,\mathbf{w}_0$, for any complex constant c, achieve the same probability of detection. Hence, any solution can be normalized to unit norm and the problem (16) is equivalent to

$$\min_{\mathbf{w}} \frac{Q^{-1}(\delta)2\sqrt{N\mathbf{w}^H\mathbf{w}+\frac{2N\alpha_2 E_x \mathbf{w}^H\mathbf{H}_2\mathbf{H}_2^H\mathbf{w}}{\sigma_n^2 N_{T2}}} - \frac{2N\alpha_1 E_x \mathbf{w}^H\mathbf{H}_1\mathbf{H}_1^H\mathbf{w}}{\sigma_n^2 N_{T1}}}{2\sqrt{N\mathbf{w}^H\mathbf{w}+\frac{2NE_x}{\sigma_n^2}\left(\frac{\alpha_1\mathbf{w}^H\mathbf{H}_1\mathbf{H}_1^H\mathbf{w}}{N_{T1}}+\frac{\alpha_2\mathbf{w}^H\mathbf{H}_2\mathbf{H}_2^H\mathbf{w}}{N_{T2}}\right)}} \quad \text{subject to} \quad \mathbf{w}^H\mathbf{w}=1. \tag{17}$$

It is not easy to obtain the global minimum of (17). In order to identify suboptimal solutions, the terms are rearranged and the problem is expressed as

$$\min_{\mathbf{w}} \frac{Q^{-1}(\delta)2\sqrt{\frac{2N\alpha_1 E_x}{\sigma_n^2 N_{T1}}\mathbf{w}^H\left(\frac{\sigma_n^2 N_{T1}\mathbf{I}}{2\alpha_1 E_x}+\frac{\alpha_2 N_{T1}\mathbf{H}_2\mathbf{H}_2^H}{\alpha_1 N_{T2}}\right)\mathbf{w}}}{2\sqrt{\frac{2N\alpha_1 E_x}{\sigma_n^2 N_{T1}}\left(\mathbf{w}^H\left(\frac{\sigma_n^2 N_{T1}\mathbf{I}}{2\alpha_1 E_x}+\frac{\alpha_2 N_{T1}\mathbf{H}_2\mathbf{H}_2^H}{\alpha_1 N_{T2}}\right)\mathbf{w}+\mathbf{w}^H\mathbf{H}_1\mathbf{H}_1^H\mathbf{w}\right)}} - \frac{\frac{2N\alpha_1 E_x \mathbf{w}^H\mathbf{H}_1\mathbf{H}_1^H\mathbf{w}}{\sigma_n^2 N_{T1}}}{2\sqrt{\frac{2N\alpha_1 E_x}{\sigma_n^2 N_{T1}}\left(\mathbf{w}^H\left(\frac{\sigma_n^2 N_{T1}\mathbf{I}}{2\alpha_1 E_x}+\frac{\alpha_2 N_{T1}\mathbf{H}_2\mathbf{H}_2^H}{\alpha_1 N_{T2}}\right)\mathbf{w}+\mathbf{w}^H\mathbf{H}_1\mathbf{H}_1^H\mathbf{w}\right)}} \quad \text{subject to} \quad \mathbf{w}^H\mathbf{w}=1. \tag{18}$$

Finally, the problem can be put in the form

$$\min_{\mathbf{w}} \; Q^{-1}(\delta)\sqrt{\frac{1}{1+R(\mathbf{w})}} - \sqrt{\frac{N\alpha_1 E_x \mathbf{w}^H\mathbf{H}_1\mathbf{H}_1^H\mathbf{w}}{2\sigma_n^2 N_{T1}}}\sqrt{\frac{R(\mathbf{w})}{1+R(\mathbf{w})}} \quad \text{subject to} \quad \mathbf{w}^H\mathbf{w}=1, \tag{19}$$

where

$$R(\mathbf{w}) = \frac{\mathbf{w}^H\mathbf{H}_1\mathbf{H}_1^H\mathbf{w}}{\mathbf{w}^H\left(\frac{\sigma_n^2 N_{T1}\mathbf{I}}{2\alpha_1 E_x}+\frac{\alpha_2 N_{T1}\mathbf{H}_2\mathbf{H}_2^H}{\alpha_1 N_{T2}}\right)\mathbf{w}}. \tag{20}$$

In this work, we do not solve for the global minimum of (19). However, suboptimal solutions that provide a reasonable performance gain are identified from (19). $R(\mathbf{w}) \geq 0$ holds as $R(\mathbf{w})$ is the ratio of quadratic forms with a positive semidefinite matrix and a positive definite matrix, respectively. For $x \geq 0$, functions $\sqrt{(1+x)^{-1}}$ and $\sqrt{x(1+x)^{-1}}$ are monotonically decreasing and monotonically increasing, respectively. This is true because the square root is a monotonically increasing function, $\frac{d}{dx}(1+x)^{-1} = -(1+x)^{-2} < 0$ and $\frac{d}{dx}x(1+x)^{-1} = (1+x)^{-2} > 0$. Thus, maximizing $R(\mathbf{w})$ subject to the constraint achieves the global minimum of the first term of the cost function. The second term of the cost function is the product of two terms. The second term of this product is also maximized by maximizing $R(\mathbf{w})$. Maximization of the first part of the product requires maximizing the quadratic form $\mathbf{w}^H\mathbf{H}_1\mathbf{H}_1^H\mathbf{w}$. Since $\mathbf{w}^H\mathbf{H}_1\mathbf{H}_1^H\mathbf{w}$ is the numerator of $R(\mathbf{w})$, the solution which maximizes $R(\mathbf{w})$ will have a non-zero component in the column space of $\mathbf{H}_1\mathbf{H}_1^H$. If $\frac{\sigma_n^2}{2} \gg \frac{\alpha_2 E_x}{N_{T2}}$, referred to as the low signal-to-noise ratio (SNR) regime, the effect of $\mathbf{w}^H\mathbf{H}_2\mathbf{H}_2^H\mathbf{w}$ in the denominator of $R(\mathbf{w})$ is negligible and the solution of maximizing $R(\mathbf{w})$ approaches the one that maximizes $\mathbf{w}^H\mathbf{H}_1\mathbf{H}_1^H\mathbf{w}$. This solution approaches the global optimum. If $\frac{\sigma_n^2}{2} \ll \frac{\alpha_2 E_x}{N_{T2}}$, referred to as the high SNR regime, the influence of $\mathbf{w}^H\mathbf{H}_2\mathbf{H}_2^H\mathbf{w}$ becomes significant and it is not possible to simultaneously maximize both terms of the product in the second term of the cost function. However, maximizing $\mathbf{w}^H\mathbf{H}_1\mathbf{H}_1^H\mathbf{w}$ is also a reasonable option, as it is also the numerator of $R(\mathbf{w})$. In the low SNR regime, this approach and maximizing $R(\mathbf{w})$ provide similar performance. If the knowledge of $\mathbf{H}_1\mathbf{H}_1^H$ is not available, a pragmatic solution is that minimizing $\mathbf{w}^H\mathbf{H}_2\mathbf{H}_2^H\mathbf{w}$. This can provide a reasonable performance in the high SNR regime as it tends to increase the value of $R(\mathbf{w})$, especially if $\mathbf{H}_2\mathbf{H}_2^H$ has a zero eigenvalue, which is guaranteed if $N_R > N_{T2}$.

Maximization of $R(\mathbf{w})$ subject to $\mathbf{w}^H\mathbf{w} = 1$ is the well-known maximum generalized Rayleigh quotient problem and the solution, denoted as $\mathbf{w}_{MRQ}$, is the eigenvector corresponding to the largest eigenvalue of the matrix $\left(\frac{\sigma_n^2 N_{T1}\mathbf{I}}{2\alpha_1 E_x}+\frac{\alpha_2 N_{T1}\mathbf{H}_2\mathbf{H}_2^H}{\alpha_1 N_{T2}}\right)^{-1}\mathbf{H}_1\mathbf{H}_1^H$. The solution that maximizes $\mathbf{w}^H\mathbf{H}_1\mathbf{H}_1^H\mathbf{w}$ subject to $\mathbf{w}^H\mathbf{w}=1$, denoted as $\mathbf{w}_{ME1}$, is the eigenvector corresponding to the largest eigenvalue of $\mathbf{H}_1\mathbf{H}_1^H$. $\mathbf{w}_{ME2}$ minimizes $\mathbf{w}^H\mathbf{H}_2\mathbf{H}_2^H\mathbf{w}$ subject to $\mathbf{w}^H\mathbf{w}=1$ and is equal to the eigenvector corresponding to the smallest eigenvalue of $\mathbf{H}_2\mathbf{H}_2^H$. Finally, we note that the detection probability can be further improved by increasing N.

IV. Likelihood Ratio Test

For given channel states, the LRT maximizes the probability of detection for a fixed probability of false alarm [11][12]. The test is based on the ratio of joint PDFs of samples $\boldsymbol{y} = [\mathbf{y}_1^T, ..., \mathbf{y}_N^T]^T$ under $H_1^{'}$ and H_2 and is given by

$$L = \frac{p(\boldsymbol{y}|H_2)}{p(\boldsymbol{y}|H_1^{'})} \quad \text{Decide } H_2 \text{ if } L > t. \tag{21}$$

Given the modulation signal set $\mathcal{X}_{2m}$ of BS2 and the channel state, the received vectors $\mathbf{y}_k$ under $H_1^{'}$ have a multivariate complex Gaussian mixture PDF,

$$\begin{aligned} p(\mathbf{y}_k|\sqrt{\alpha_2}\,\mathbf{H}_2, \mathcal{X}_{2m}, H_1^{'}) &= \sum_{\mathbf{x}_{2i} \in \mathcal{X}_{2m}^{N_{T2}}} P(\mathbf{x}_{2i}) f_{\mathbf{n}}(\mathbf{y}_k - \sqrt{\alpha_2}\,\mathbf{H}_2\mathbf{x}_{2i}) \\ &= \frac{1}{|\mathcal{X}_{2m}|^{N_{T2}}} \sum_{\mathbf{x}_{2i} \in \mathcal{X}_{2m}^{N_{T2}}} f_{\mathbf{n}}(\mathbf{y}_k - \sqrt{\alpha_2}\,\mathbf{H}_2\mathbf{x}_{2i}), \end{aligned} \tag{22}$$

where $f_{\mathbf{n}}(\mathbf{u}) = \frac{1}{(\pi\sigma_n^2)^{N_R}} \exp(-\frac{\mathbf{u}^H\mathbf{u}}{\sigma_n^2})$ is the PDF of $\mathbf{n} \sim \mathcal{CN}(0, \sigma_n^2\mathbf{I})$ and $|\mathcal{X}_{2m}|$ represents the cardinality of $\mathcal{X}_{2m}$.

Using the fact that in LTE the transmission format does not change within a PRB and assuming independent symbols, the joint probability density can be written as

$$p(\boldsymbol{y}|\sqrt{\alpha_2}\,\mathbf{H}_2, \mathcal{X}_{2m}, H_1^{'}) = \prod_{k=1}^{N} p(\mathbf{y}_k|\sqrt{\alpha_2}\,\mathbf{H}_2, \mathcal{X}_{2m}, H_1^{'}). \tag{23}$$

Typically, UEs are only aware of modulation formats of their own data. Hence, when UEs are sensing PRBs which are not carrying their data, the modulation format is unknown. Thus the modulation format is unknown in general and the final joint PDF is obtained by averaging over all M possible modulation formats,

$$p(\boldsymbol{y}|H_1^{'}) = \frac{1}{M} \sum_{m=1}^{M} \prod_{k=1}^{N} p(\mathbf{y}_k|\sqrt{\alpha_2}\mathbf{H}_2, \mathcal{X}_{2m}, H_1^{'}). \tag{24}$$

Similarly, under H_2 we obtain

$$\begin{aligned} p(\mathbf{y}_k|\sqrt{\alpha_1}\,\mathbf{H}_1, \sqrt{\alpha_2}\,\mathbf{H}_2, \mathcal{X}_{1m}, \mathcal{X}_{2l}, H_2) &= \frac{1}{|\mathcal{X}_{1m}|^{N_{T1}}|\mathcal{X}_{2m}|^{N_{T2}}} \\ &\times \sum_{\mathbf{x}_{1i} \in \mathcal{X}_{1m}^{N_{T1}}, \mathbf{x}_{2j} \in \mathcal{X}_{2l}^{N_{T2}}} f_{\mathbf{n}}(\mathbf{y}_k - \sqrt{\alpha_1}\,\mathbf{H}_1\mathbf{x}_{1i} - \sqrt{\alpha_2}\,\mathbf{H}_2\mathbf{x}_{2j}) \end{aligned} \tag{25}$$

where $\mathcal{X}_{1m}$ is the modulation symbol set of BS1. Finally, averaging over the different modulation formats, we obtain,

$$\begin{aligned} p(\boldsymbol{y}|H_2) &= \frac{1}{M^2} \\ &\times \sum_{m=1}^{M} \sum_{l=1}^{M} \prod_{k=1}^{N} p(\mathbf{y}_k|\sqrt{\alpha_1}\,\mathbf{H}_1, \sqrt{\alpha_2}\,\mathbf{H}_2, \mathcal{X}_{1m}, \mathcal{X}_{2l}, H_2). \end{aligned} \tag{26}$$

We choose $M = 3$ with $\mathcal{X}_{r1} = 4$QAM, $\mathcal{X}_{r2} = 16$QAM and $\mathcal{X}_{r3} = 64$QAM, $r \in \{1, 2\}$ for the system under investigation, since these are the most relevant modulation formats for LTE.

V. Performance Results

Simulations have been performed to compare the different methods. All the results have been averaged over 2000 small-scale fading channel realizations. We choose $N_{T1} = N_{T2} = 1$, $N_R = 2$ and $E_x = 1$. Assuming an approximate overhead of 29% from control channels and reference signals, and taking into account that sensing is performed over a single PRB a value of $N = 120$ is chosen. Simulations are performed under the signal-to-interference ratio (SIR) and SNR conditions of ($\frac{\alpha_1}{\alpha_2} = -6$ dB, $\frac{\alpha_2}{\sigma_n^2} = 10$ dB) and ($\frac{\alpha_1}{\alpha_2} = -6$ dB, $\frac{\alpha_2}{\sigma_n^2} = 0$ dB).

The performance of detectors is captured by the receiver operating characteristics (ROC) curve which is the probability of detection depicted versus the probability of false alarm [11]. Figure 2 provides the ROC for the different methods under perfect channel estimation. For $\frac{\alpha_2}{\sigma_n^2} = 10$ dB, the LRT performs best and achieves nearly 100% detection probability at a false alarm probability of 10%. Even though the LRT is of huge complexity, it serves as a useful benchmark for performance comparisons. In ED, the $\mathbf{w}_{MRQ}$ solution performs best with $P_d = 97\%$ at $P_f = 10\%$. The $\mathbf{w}_{ME2}$ solution performs close to $\mathbf{w}_{MRQ}$ and is slightly better than the $\mathbf{w}_{ME1}$ solution at low values of P_f. All the beamforming methods outperform the EGC method in this setting. For $\frac{\alpha_2}{\sigma_n^2} = 0$ dB, the LRT performs better than the energy detectors for $P_f \geq 10\%$. $\mathbf{w}_{MRQ}$ is slightly better than the LRT at $P_f = 5\%$. This is due to the fact that the LRT discussed here does not use a channel dependent threshold which maintains the target false alarm probability at every channel state. Calculation of such a threshold requires the knowledge of the PDF of the likelihood ratio under the hypothesis $H_1^{'}$. This is not pursued in this paper. However, the threshold that guarantees a target average probability of false alarm can be easily obtained from simulations. For the energy detectors, the thresholds computed using (8) and (14) maintain the target false alarm probability at every channel state. Among energy detectors, there is a significant gain for both $\mathbf{w}_{MRQ}$ and $\mathbf{w}_{ME1}$ compared to $\mathbf{w}_{ME2}$ and the EGC. This is expected as the conditions become closer to the low SNR regime. For comparison, the performance of a single antenna ED is also shown, which is considerably worse when compared to the multi-antenna energy detectors.

To study the impact of channel estimation, we adopt an AWGN error model. Let $[\mathbf{A}]_{m,n}$ denote the element at the mth row and the nth column of a matrix $\mathbf{A}$ and $\mathbf{H}_{ik}$ denote the channel matrix, at resource element k, with respect to the ith BS. The estimate of the value $[\mathbf{H}_{ik}]_{m,n}$ is modeled as $[\mathbf{H}_{ik}]_{m,n} = [\mathbf{H}_i]_{m,n} + v_{k,m,n}$, where $v_{k,m,n} \sim \mathcal{CN}(0, \sigma^2_{\text{nmse},i})$ and $\sigma^2_{\text{nmse},i}$ is the normalized mean square error of the estimator. $v_{k,m,n}$ is assumed to be independent in k, m and n directions. The normalized mean square error is computed based on the CRS-LS curves of [14] for ITU PedB and a speed of 0 km/h. Specifically, the normalized mean square error follows $\log(\sigma^2_{\text{nmse},i}) = -\frac{\text{SINR}_i(\text{dB})}{10} - 0.26$, where $\text{SINR}_i(\text{dB}) = 10\log\left(\frac{\alpha_i}{\alpha_1+\alpha_2+\sigma_n^2-\alpha_i}\right)$. The beamforming vectors are computed by replacing the parameters, $\mathbf{H}_i\mathbf{H}_i^H$, by their estimates $\widehat{\mathbf{H}_i\mathbf{H}_i^H}$, obtained as $\widehat{\mathbf{H}_i\mathbf{H}_i^H} = \frac{1}{N}\sum_{k=1}^{N} \mathbf{H}_{ik}\mathbf{H}_{ik}^H$. Similarly, for EGC, the parameter involved in (8) is estimated as $\frac{1}{N}\sum_{k=1}^{N}\sum_{m=1}^{N_R} \mathbf{h}_{2m,k}^H\mathbf{h}_{2m,k}$, where $\mathbf{h}_{2m,k}$ is the mth column of the estimated channel matrix $\mathbf{H}_{2k}^T$. However, due to estimation errors, the thresholds computed from (8) and (14) cannot

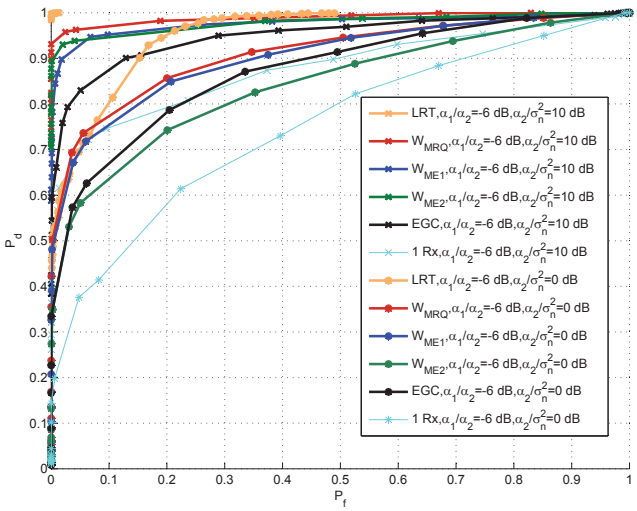

Fig. 2. Receiver operating characteristics with ideal channel estimation.

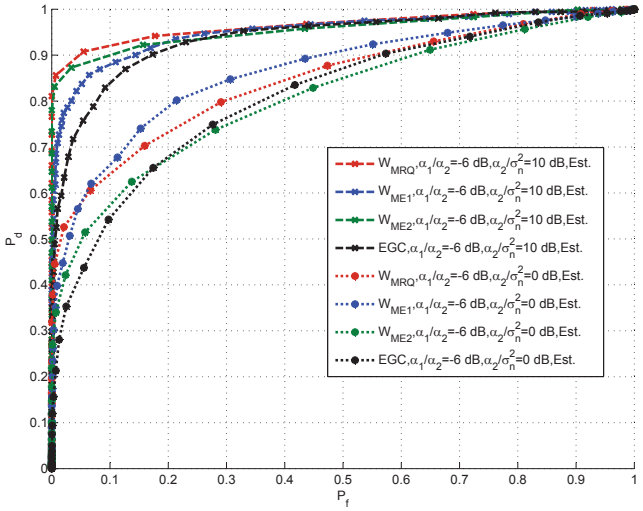

Fig. 3. Receiver operating characteristics with channel estimation errors.

ensure the target false alarm probability at every channel state and hence cannot meet the target average probability of false alarm. To be able to achieve a desired false alarm probability, we modify the threshold calculation as $t_{EGC} = t_1 + (\nu + \lambda_1)$ and $t_{BF} = t_2 + (u + \lambda_3)$. In [5], under ideal channel estimates, the performance loss incurred from adopting such a threshold was shown to be negligible for practical values of target false alarm probabilities. In the presence of estimation errors, the values of t_1 and t_2 for a desired average false alarm probability can be easily found from simulations. A mathematical analysis of the same is left for a future study. Figure 3 provides the ROC in the presence of channel estimation errors while employing the modified threshold. The detection probability of all the schemes suffers from a loss due to estimation errors. For $\frac{\alpha_2}{\sigma_n^2} = 10$ dB ($\text{SINR}_1 = -6.4$ dB and $\text{SINR}_2 = 4.5$ dB) the performance loss at $P_f = 10\%$ for the different schemes is less than 0.1. $\mathbf{w}_{MRQ}$ performs best in this setting. $\mathbf{w}_{ME2}$ performs better than $\mathbf{w}_{ME1}$ because the estimation error in the serving cell channel is much lower than that of the other cell channel. At the low SNR setting of $\frac{\alpha_2}{\sigma_n^2} = 0$ dB ($\text{SINR}_1 = -9$ dB and $\text{SINR}_2 = -0.9$ dB) the estimation errors in both serving cell channel and other cell channel increase when compared to that of the high SNR setting, with the serving cell channel suffering the larger increase. As a result $\mathbf{w}_{MRQ}$ and EGC suffer a loss of nearly 0.15 at $P_f = 10\%$ and $\mathbf{w}_{ME1}$ performs better than $\mathbf{w}_{MRQ}$.

VI. CONCLUSION

We have studied the problem of sensing in the presence of a desired signal using multiple receive antennas in the context of LTE-A systems. Energy detectors based on equal gain combining and beamforming are analyzed. The optimization problem for the design of beamformers is developed and suboptimal solutions are identified. The behavior of the different beamformers under the low and high SNR regimes are analyzed. It is shown that the beamforming based detectors achieve a significant performance gain compared to the equal gain combining based detector under ideal channel estimates as well as realistic channel estimates. It is also shown that a reasonable detection performance can be obtained even with a realistic channel estimation.

REFERENCES

[1] M. Song, C. Xin, Y. Zhao and X. Cheng, "Dynamic spectrum access: from cognitive radio to network radio", *IEEE Wireless Commun.*, February 2012.

[2] I.F. Akyildiz, W.Y. Lee, M.C. Vuran and S. Mohanty, "NeXt generation/dynamic spectrum access/cognitive radio wireless networks: A survey", *Computer Networks*, vol. 50, issue 13, September 2006.

[3] H. Bagheri, H. Chowdhury, T. Bräysy, P. Ahokangas and M. Katz, "Business model for mobile clouds-based rich content distribution", *Proc. 10th Int. Symp. on Wireless Comm. Systems*, August 2013.

[4] J. Markendahl, Ö. Mäkitalo, B.G. Mölleryd and J. Werding, "Mobile broadband expansion calls for more spectrum or base stations - analysis of the value of spectrum and the role of spectrum aggregation", *21st European Regional ITS Conference*, Copenhagen 2010.

[5] P. Karunakaran, T. Wagner, A. Scherb and W.H. Gerstacker, "Sensing for spectrum sharing in cognitive cellular networks", *accepted for presentation at IEEE Wireless Comm. and Networking Conference*, WCNC, available at arxiv.org, April 2014.

[6] S. Sesia, I. Toufik and M. Baker, *LTE - The UMTS long term evolution: From theory to practice*, 2nd ed., Wiley, 2011.

[7] T. Yucek, and H. Arslan, "A survey of spectrum sensing algorithms for cognitive radio applications", *IEEE Commun. Surveys & Tutorials*, 2009.

[8] W. Lee and D.H. Cho, "Enhanced spectrum sensing scheme in cognitive radio systems with MIMO antennae", *IEEE Trans. on Vehicular Technology*, vol.60, March 2011.

[9] F. Moghimi, R.K. Mallik and R. Schober, "Sensing time and power optimization in MIMO cognitive radio networks", *IEEE Trans. Wireless Commun.*, vol.11, September 2012.

[10] F.F. Digham, M.S. Alouini and M.K. Simon, "On the energy detection of unknown signals over fading channels", *IEEE International Conference on Communications*, ICC '03, May 2003.

[11] S.M. Kay, *Fundamentals of statistical signal processing: Detection theory*, NJ: Prentice Hall, 1998.

[12] A. Whalen, "Statistical theory of signal detection and parameter estimation", *IEEE Commun. Mag.*, vol.22, June 1984.

[13] J.G. Proakis, *Digital communications*, 4th ed., McGraw-Hill, 2001.

[14] M. Meidlinger and Q. Wang "Performance evaluation of LTE advanced downlink channel estimators", *Proc. of Int. Conf. on Systems, Signals and Image Processing*, IWSSIP, April 2012.